J. Membrane Biol. 122, 177–187 (1991)
002226319100091X

The Journal of
Membrane Biology

Analysis and Use of the Perforated Patch Technique for Recording Ionic Currents in Pancreatic β-Cells

Salvador Sala, Ramin V. Parsey, Akiva S. Cohen, and Donald R. Matteson
Department of Biophysics, University of Maryland, Baltimore, Maryland 21201

Summary. We have used the nystatin perforated patch technique to study ionic currents in rat pancreatic β-cells. The access resistance (R_a) between the pipette and the cell cytoplasm, measured by analyzing capacitive currents, decreased with a slow exponential time course (τ = 5.4 ± 2.7 min) after seal formation. As R_a decreased, the magnitude of voltage-dependent K and Ca currents increased with a similar time course, and their activation kinetics became faster. After R_a stabilized, the macroscopic currents remained stable for up to an hour or more. When the final R_a was sufficiently low, Ca tail currents could be resolved which had properties similar to those recorded with the classical whole-cell technique. Two types of K channels could be characterized with perforated patch recordings of macroscopic K currents: (i) ATP-blockable K (K_{ATP}) channels which generate a time and voltage independent current that is blocked by glyburide and enhanced by pinacidil and (ii) voltage-dependent K (K_v) channels. Whole-cell recordings of K_{ATP} currents in the absence of ATP in the pipette showed that the maximum K_{ATP} conductance of the β-cell was 83.8 ± 40 nS. Perforated patch recordings show that the resting K_{ATP} conductance is 3.57 ± 2.09 nS, which corresponds to about 4% of the channels being open in the intact β-cell. In classical whole-cell recordings, K_v activation kinetics become faster during the first 10–15 min of recording, probably due to a dissipating Donnan potential. In perforated patch recordings where the Donnan potential is very small, K_v activation kinetics were nearly identical to the steady-state whole cell measurements.

Key Words perforated-patch · nystatin · patch clamp · β-cell · K channel · Ca channel

Introduction

One of the most powerful techniques used in the electrophysiological study of cells is the whole cell variant of the patch-clamp technique (Hamill et al., 1981). Proper implementation of this method provides a high resistance seal between the glass electrode and the cell membrane, along with a low resistance access to the cell interior. The main disadvantage of the technique concerns the loss of the soluble constituents of the cell through the patch electrode. This dialysis or washout has been cited as a possible explanation for the loss of cellular responsiveness to known stimulants (Lucero & Pappone, 1990), the diminution or "rundown" of Ca currents (Hagiwara & Byerly, 1983), or the slow shift in voltage-dependent processes due to a slowly diffusing Donnan potential (Marty & Neher, 1983; Fernandez, Fox & Krasne, 1984; Cahalan et al., 1985; Cota, 1986).

Recently, using the on-cell configuration of the patch-clamp technique, attempts have been made to permeabilize the membrane under the electrode tip with pores permeable to small ions. Ideally this would allow electrical access to the cell interior without the washout of larger molecules. Lindau and Fernandez (1986), using 400 μM ATP in the pipette as the pore-forming agent, reduced the loss of stimulus-secretion coupling in mast cells but reported access resistances in the 200 to 5000 MΩ range. Horn and Marty (1988) greatly improved the technique by using the pore-forming agent nystatin, and achieved access resistances in the 4–50 MΩ range. With this "perforated patch" technique Ca-activated K and Cl currents responded to activation of muscarinic receptors for up to 1 hr, in contrast to only 5 min with the classical whole-cell technique (Horn & Marty, 1988). Several investigators have now used the nystatin perforated patch technique to reduce Ca current rundown and to study membrane events that require an intact cytoplasm for expression (Falke et al., 1989; Korn & Horn, 1989; Kurachi et al., 1989; Lucero & Pappone, 1990).

The purpose of our study was to examine the nystatin perforated patch technique in detail and to use it to record macroscopic currents from isolated rat pancreatic β-cells. The perforated patch technique will likely be an extremely useful tool for studying stimulus-secretion coupling in the pancreatic β-cell because it allows accurate whole-cell measurements while leaving the internal cellular envi-

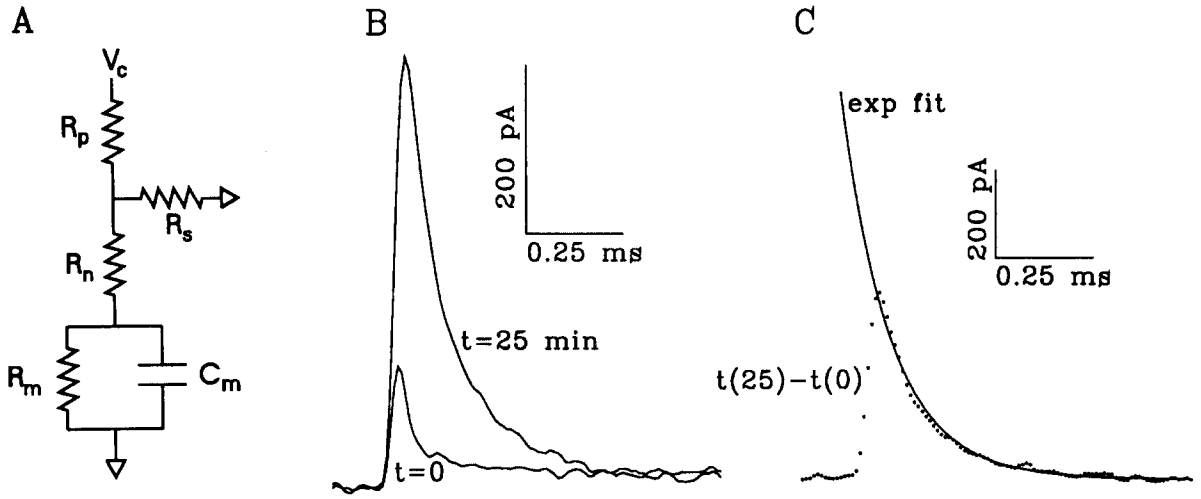

Fig. 1. Procedure for measuring the total access resistance (R_a). (*A*) Equivalent circuit of the nystatin perforated patch configuration. The components represent the pipette resistance (R_p), seal resistance (R_s), nystatin perforated patch resistance (R_n), cell membrane resistance (R_m) and cell capacitance (C_m). V_c is the command voltage. (*B*) These currents were generated by 5 msec steps of − 10 mV, and the current was sampled at 100 kHz. The trace labeled $t = 0$ was recorded immediately after seal formation, and $t = 25$ was recorded 25 min later after nystatin perforations had developed. (*C*) The dotted trace labeled *t(25)-t(0)* is the difference between the two traces shown in *B*, and it is the current required to charge the cell capacitance through R_p and R_n. The smooth curve (labeled exp fit) is the fit of a single exponential to the difference record

ronment undisturbed. A preliminary report of these results has appeared (Cohen et al., 1990).

Materials and Methods

Cell Culture

The pancreas was excised from adult male Sprague-Dawley rats anesthetized with Nembutal (1 ml/kg body weight). The tissue was minced and washed in Hank's Balanced Salt Solution (HBSS) containing 5 mg/ml bovine serum albumin (BSA) and then digested with Type IV collagenase at 37°C for approximately 1 hr. Islets were washed several times in HBSS and then picked by hand using a Lang-Levi pipette. The islets were then dispersed by mechanical agitation in a Spinner solution containing 1 mM EGTA and 10 mg/ml BSA. Cells were washed in RPMI 1640 media with 10 mg/ml BSA several times and then plated on coverslips in final culture media (RPMI supplemented with 10% fetal bovine serum, 1% glutamine, 100 U/ml penicillin and 100 μg/ml streptomycin). Cells were maintained at 37°C in 5% CO_2 and used for up to one week. All of the culture solutions were made with salts obtained from Sigma. We have previously shown that about 89% of the dispersed cells cultured in this way are insulin-secreting β-cells (Hiriart & Matteson, 1988). Thus, the majority of cells recorded from in this study were β-cells, although no attempt was made to identify individual cells.

Access Resistance Calculation

Our method of determining the access resistance (R_a) between the pipette and the cell interior is illustrated in Fig. 1. An equivalent circuit of the perforated patch configuration is shown in Fig. 1*A*. In this circuit a step change in the command voltage (V_c) produces an exponentially decaying current in the patch electrode (I_p) which has a time constant (τ_a) given by the following:

$$\tau_a = \frac{C_m\left[R_p + R_n\left(1 + \frac{R_p}{R_s}\right)\right]}{1 + \frac{R_p}{R_s} + \frac{R_p}{R_m} + \frac{R_n}{R_m}\left(1 + \frac{R_p}{R_s}\right)} \quad (1)$$

where C_m is the membrane capacitance and R_p, R_s, R_m and R_n are the resistances of the pipette, seal, membrane and perforated patch, respectively. R_p is usually much smaller than either R_s or R_m, therefore τ_a becomes

$$\tau_a = \frac{C_m(R_p + R_n)}{1 + \frac{R_n}{R_m}}. \quad (2)$$

If R_n is much less than R_m then τ_a/C_m gives an estimate of the total R_a (which is equal to $R_p + R_n$). If R_n is large compared to R_m, τ_a/C_m underestimates the access resistance by the factor $(1 + R_n/R_m)$. This underestimate would be significant only in the early stages of nystatin action, when the perforated patch resistance is large.

In order to measure τ_a and C_m, we obtained records of the current required to discharge C_m. These were obtained by subtracting an I_p recorded immediately after sealing (Fig. 1*B*, $t = 0$) from an I_p recorded later (e.g., $t = 25$). The early record is measured before nystatin perforations develop and is thus due primarily to the electrode capacitance and stray capacitance to ground. As nystatin perforations develop, there is an increase in the magnitude of I_p. The subtracted record ($t(25)$-$t(0)$) reflects the charging of C_m through the access resistance. By integrating this current we can get the total charge (Q) required to change the

Table. Composition of Solutions

External Solutions					
Solution	NaCl	$CaCl_2$	KCl	$MgCl_2$	HEPES
A	114[a]	2	30	2	10
B	136	10	—	—	10

Internal Solutions									
Solution	CsCl	Cs_2SO_4	CsGlu	KGlu	$MgCl_2$	KCl	K_2SO_4	EGTA	HEPES
C	55	70	—	—	7	—	—	—	10
D	30	—	100	—	2	—	—	10	10
E	—	—	—	—	7	55	70	—	10
F	—	—	—	100	2	30	—	10	10

[a] All concentrations are in mM.

membrane potential by V mV, and by fitting an exponential to the current we obtained the time constant (τ_a). R_a was then calculated using the relationships $C_m = Q/V$ and $R_a = \tau_a/C_m$. We tested this method on a model of the circuit shown in Fig. 1*A* using R_p = 1 MΩ, $R_s = R_m$ = 1000 MΩ, R_n = 10 MΩ and C_m = 10 pF and obtained 11.4 MΩ for τ_a/C_m, which is close to the total access resistance of 11 MΩ.

Electrodes

Patch electrodes were pulled from either soda-lime glass or Corning N51A borosilicate glass and fire-polished before use. In an attempt to minimize R_a in perforated patch experiments we made steeply tapered, large diameter electrodes using soda-lime glass. Electrode resistances varied from 0.5 to 2 MΩ. In nystatin experiments, the electrodes were quickly dipped into a nystatin free internal solution immediately before use, and then back-filled with the nystatin containing solution. Positive pressure was applied briefly while moving the electrode through the air/water interface and then discontinued.

Solutions

The compositions of all solutions are shown in the Table. Two external solutions were prepared: solution A for measuring potassium currents and solution B for measuring calcium currents. The pH of both solutions was adjusted to 7.40. Internal solutions C and E were modelled after those in Korn and Horn (1989) for perforated patch experiments and were designed to minimize the Donnan potential created by large impermeant intracellular anions. With these solutions, and assuming an intracellular impermeant anion concentration of 100 mM, the Donnan potential would be about 2 mV with the cell negative to the pipette (*cf.* Horn & Marty, 1988). The pH of the internal solutions was 7.30. A 10 mM stock solution of glyburide (Sigma) was made up in dimethyl sulfoxide (DMSO) and subsequently diluted in external solution A just before use. A 50 mM stock solution of pinacidil (a gift from Lilly Research Laboratories, Indianapolis, IN) was made in 0.05 N HCl and diluted in external solution A for use.

A nystatin (Sigma) stock solution of 25 mg/ml in DMSO was stored at −4°C in the dark for up to one week. This stock solution was diluted in the appropriate filtered internal solution to give a final nystatin concentration of 100 μg/ml and sonicated briefly to ensure proper dispersion. This final solution was kept in the dark at room temperature and used for up to 5 hr.

Pluronic (Molecular Probes) stock solution was made by dissolving 25 mg in 1 ml of DMSO at 37°C for 10 min. Stock solution was stored at −4°C and used for up to 1 month. This stock was diluted to a final concentration of 0.05% in the internal solution containing 100 μg/ml nystatin and used as soon as possible. When using pluronic, it was not necessary to sonicate the solution. In control experiments, pipette solutions containing DMSO and pluronic alone did not produce the changes in capacitive current indicative of nystatin action (*see* Results).

Data Acquisition and Analysis

Two patch-clamp configurations were used to record macroscopic currents: the classical whole cell configuration described by Hamill et al. (1981) and the nystatin perforated patch technique of Horn and Marty (1988). Voltage-clamp pulses were applied with a programmable 14 bit D/A converter. The output of the voltage clamp was filtered at 10 kHz with an 8-pole Bessel filter and sampled at rates up to 100 kHz with a 16 bit A/D converter. The patch clamp and computer interface were designed and built in our lab. Data acquisition and analysis were done on a Compaq 386 computer using software written in C. All experiments were done at room temperature (22–24°C). The holding potential was −80 mV unless otherwise indicated.

When used, linear leak subtraction was performed in two different ways. In all Ca current measurements and classical whole-cell measurements of voltage-dependent K currents, a P/2 procedure was used (Armstrong & Bezanilla, 1974). In other experiments where K current was measured there was often significant current through K_{ATP} channels. The open probability of these channels is voltage independent, but the single channel current voltage relationship is nonlinear (Ashcroft, Kakei & Kelly, 1989), so P/2 does not work properly. If linear leak subtraction was required in these experiments, the voltage-independent current generated by a small depolarization was scaled and subtracted from the data.

The fast and slow components of Ca tail currents were separated with a stripping procedure. First, an exponential was fit to the slow component of the tail, and the extrapolated amplitude of the exponential was used as a measure of this component. This slow exponential was then subtracted from the tail current, and the measured amplitude of the remaining current was used as a measure of the fast component.

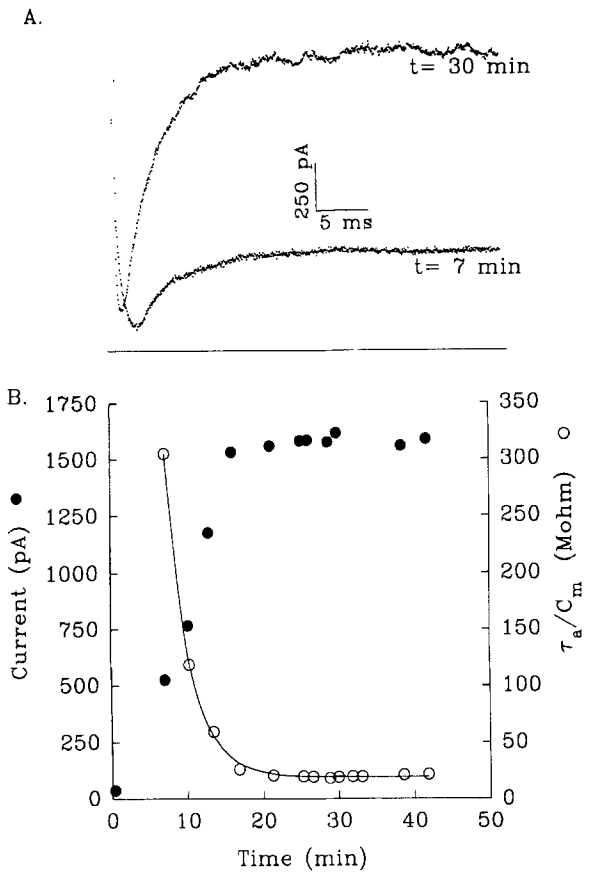

Fig. 2. Time course of stabilization of the access resistance (calculated as τ_a/C_m) and the outward K current. (*A*) K currents generated by 37 msec steps to +70 mV, 7 or 30 min after seal formation. At 30 min, the current is larger and activates more rapidly. (*B*) The maximum amplitude of the K current at +70 mV and the access resistance are plotted *vs.* time after seal formation. The smooth curve is the fit of a single exponential with a time constant of 3.0 min. The access resistance stabilized at 19.3 MΩ and the K current reached a value of 1.58 nA in approximately 35 min. Solutions used were, external solution A and internal solution E

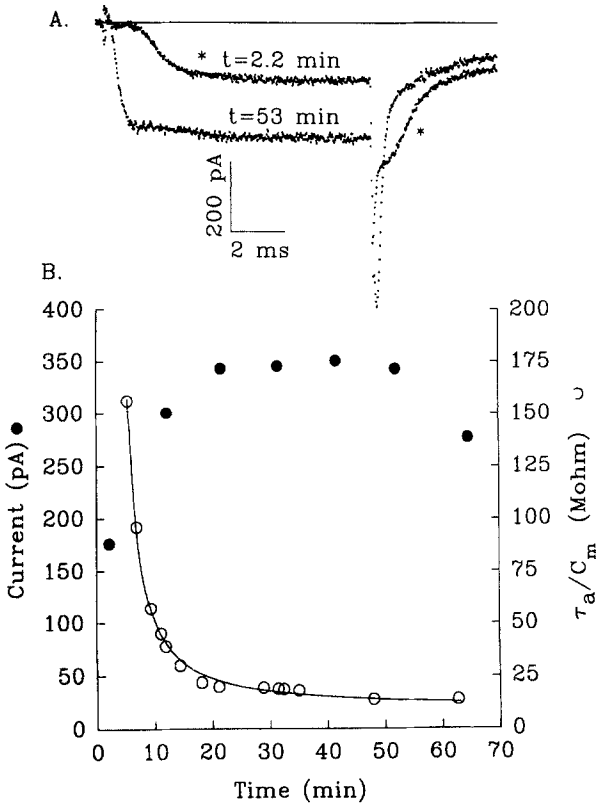

Fig. 3. (*A*) Calcium currents recorded at 2.2 and 53 min after seal formation using 10 msec steps to +10 mV from a holding potential of −80 mV. The calcium current at 53 min is nearly twice as large as the current at 2.2 min. The earlier current activates more slowly, and there is a pronounced "hump" in the tail current. (*B*) Peak calcium current and access resistance are plotted *versus* time after seal formation. The rise in calcium current amplitude and the fall in the access resistance have similar time courses. The smooth curve is the fit of an exponential function with a time constant of 3.3 min. The Ca current stabilized within 20 min and remained constant for at least 30 min. Solutions used were external solution B and internal solution C. Final R_a = 14 MΩ; C_m = 4.9 pF; τ_a = 70 μsec

In potassium channel experiments, we have used the steady-state K conductance (g_K) of the cell as a measure of K_{ATP} channel activity. The steady-state g_K was calculated by fitting a least squares regression line to the steady-state current voltage relationship over a negative voltage range (from −120 to −40 mV).

Results

Time Course of Patch Perforations by Nystatin

Our first step in analyzing the perforated patch technique was to characterize the time course and extent of the perforations, and to study the effect of changes in R_a on the measurement of voltage-dependent currents generated by the β-cells. Rat pancreatic β-cells are known to contain several populations of ionic channels; e.g. two types of Ca channels (Hiriart & Matteson, 1988; Sala & Matteson, 1990; Ashcroft, Kelly & Smith, 1990) and various types of K channels, including voltage-dependent K channels (Rorsman & Trube, 1986). In Figs. 2 and 3, we have compared changes in R_a to changes in the magnitude of either the voltage-dependent K current (Fig. 2) or the inward Ca current (Fig. 3). As shown in Figs. (2) and (3) a single exponential function provides a good fit to the time course of R_a. In experiments done in the absence of the dispersant pluronic in the pipette, the time constant of the decline in R_a averaged 5.4 ± 2.7 min (n = 17), and the steady-state level of R_a typically ranged from 5 to 20 MΩ. Several factors seem to affect this time course and its variability. For example, the use of steeply tapered electrodes

decreased the time required to equilibrate. The amount of nystatin free solution in the tip will obviously affect the time course, and should be minimized. In addition, the presence of pluronic tended to decrease the time constant, but we have not quantitated this effect.

While the nystatin perforations are developing, the amplitude and time course of the recorded K and Ca currents are changing (Fig. 2 and 3). The outward potassium current was monitored by applying 37 msec steps to +70 mV from a holding potential of −80 mV. Calcium currents were monitored in other experiments by depolarizing to +10 mV from the same holding potential. The amplitude of both the K current (Fig. 2) and the Ca current (Fig. 3) increased with approximately the same time course as the decrease in R_a, and then became stable at about the same time that R_a stabilized. The current traces in Figs. 2*A* and 3*A* also illustrate that the activation kinetics are faster when R_a decreases. The membrane currents activate faster, in part, because the membrane voltage rises more rapidly, and also because the voltage drop across the series resistance is smaller (*see* Discussion). An important consequence of the changing ionic currents is that one must wait (for up to 20–30 min) for the currents to stabilize before initiating any experimental intervention.

In order to confirm whether or not we were still in the perforated patch mode and not whole cell, we applied a brief pulse of suction of sufficient pressure to rupture the patch under the electrode. This usually produced a sharp decrease in R_a. In Ca channel experiments, a complete disappearance of Ca currents occurred within 1 to 2 min. In K channel experiments, rupturing the patch caused an increase in the holding current, presumably due to the opening of K_{ATP} channels that were being blocked by intracellular ATP (*see below*). In all experiments the cells became leaky a few minutes after break-in, probably as a result of nystatin entry into the cell and insertion into the entire cell surface.

Ca Tail Currents in Perforated Patch

In rat β-cells it has been shown that there are two types of Ca channels; a fast deactivating (FD) channel and a more slowly deactivating (SD) channel which can readily be studied using tail currents (Hiriart & Matteson, 1988). In nystatin experiments, the relatively high access resistance could prevent accurate tail current measurements due to poor temporal resolution. Therefore, we attempted to minimize R_a by using relatively large diameter, steeply tapered patch electrodes in order to measure Ca tail currents using the perforated patch configuration. These recordings were compared with whole-cell measurements. In many perforated patch experiments (e.g.,

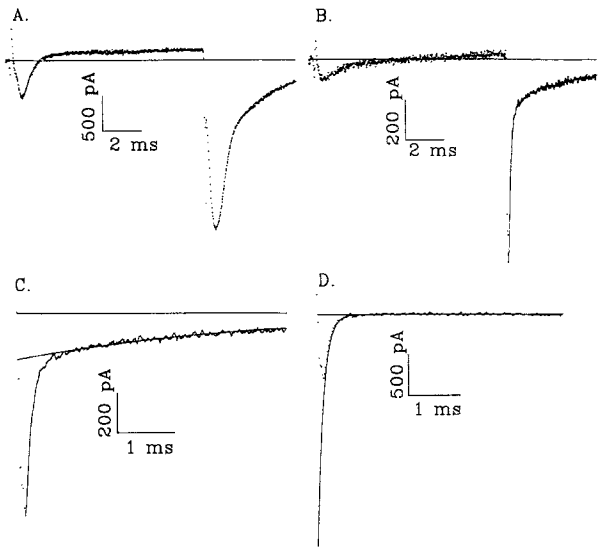

Fig. 4. Ca tail currents. (*A*) Perforated patch recording showing bad temporal resolution of tail currents. The record was taken with a 10 msec step to +10 mV from a holding potential of −80 mV. R_a = 13 MΩ; C_m = 9.3 pF; τ_a = 120 μsec. (*B*) Perforated patch record showing good temporal resolution of tail currents. The record was obtained with the same pulse protocol as in *A*. The tail current clearly consists of two components, one fast and the other slow. R_a = 5.6 MΩ; C_m = 6.6 pF; τ_a = 37 μsec. (*C*) The noisy line is the tail current from the same record as in *B*, and the solid line is an exponential fit to the slow component. (*D*) The dotted trace is the result of subtracting the slow fit from the tail. The solid line is an exponential fit to the remaining data. Note that the scale is different than in *C*. The extrapolated amplitude of this fast component is several times larger than the data. We therefore use the amplitude of the remaining current as a measure of the fast component because of the likelihood of significant extrapolation error. Solutions used were external solution B and internal solution C

Fig. 4*A*), we found that a large R_a produced a hooked or rounded tail current which was inappropriate for quantitative analysis. The time constant for charging the membrane capacitance (τ_a) was 120 μsec in the cell illustrated in Fig. 4*A*. An example of a tail current without a pronounced hook is shown in Fig. 4*B*, from a cell with a final R_a of 5 MΩ and a τ_a of 37 μsec. It is clear that the tail current is composed of both a fast and a slow deactivating component.

The voltage dependence of SD and FD Ca channel activation can be studied by analyzing Ca tail currents as shown in Fig. 4*C* and *D* (*cf.* Matteson & Armstrong, 1986; Hiriart & Matteson, 1988). The tail currents are separated into two components by a stripping routine, as described in Materials and Methods. Figure 4*C* illustrates an exponential fit of the slow component, which in this case has a time constant of 4.33 msec. The remaining fast component could be fit with a time constant of 124 μsec. In experiments with τ_a < 100 μsec, the time constants averaged 202 ± 72 μsec and 4.3 ± 0.70 msec for the

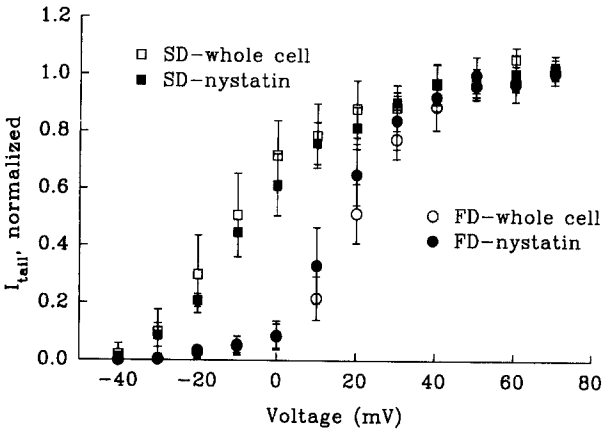

Fig. 5. Conductance-voltage relationships for fast and slow deactivating Ca channels. The normalized amplitudes of the slow and fast Ca tail currents (which are measures of the SD and FD channel conductance, respectively) are plotted *vs.* the voltage of the activating pulse. Open symbols represent data from 15 cells with classical whole cell recording, and the filled symbols are from three cells in the perforated patch configuration. Data are plotted as mean ± SD. Solutions for the perforated patch experiments were external solution B and internal solution C, and for whole cell they were external solution B and internal solution D

fast and slow components, respectively. These time constants are larger than those found using the classical whole-cell technique in rat β-cells (Hiriart & Matteson, 1988), probably due to the relatively large R_a. In Figure 5, the normalized amplitudes of the slow and fast components are plotted as a function of the activation voltage in either perforated patch or classical whole-cell experiments. In both cases, the slow component of the tail (generated by SD Ca channels) activates over a more negative voltage range than the fast component. The half-maximal voltage for the slow component is about −7 mV and about +18 mV for the fast component. Thus, the data from the perforated patch experiments closely resemble that from whole-cell.

Whole-cell K Currents and the Maximum K_{ATP} Conductance

The perforated patch technique offers distinct advantages for studying the activity of ATP-blockable K (K_{ATP}) channels in an intact β-cell, because it leaves the internal milieu of the cell intact. The use of classical whole-cell recordings (i.e., ruptured patch) of K_{ATP} channels is limited by the dialysis of the soluble components of the cell through the patch electrode, as shown in Fig. 6. The currents in Fig. 6*A*, taken with no ATP in the pipette, show that the holding current and the steady-state outward current both increase with time after break-in. The steady-state current reverses near E_K indicating that K-selective channels carry the current. The increase in

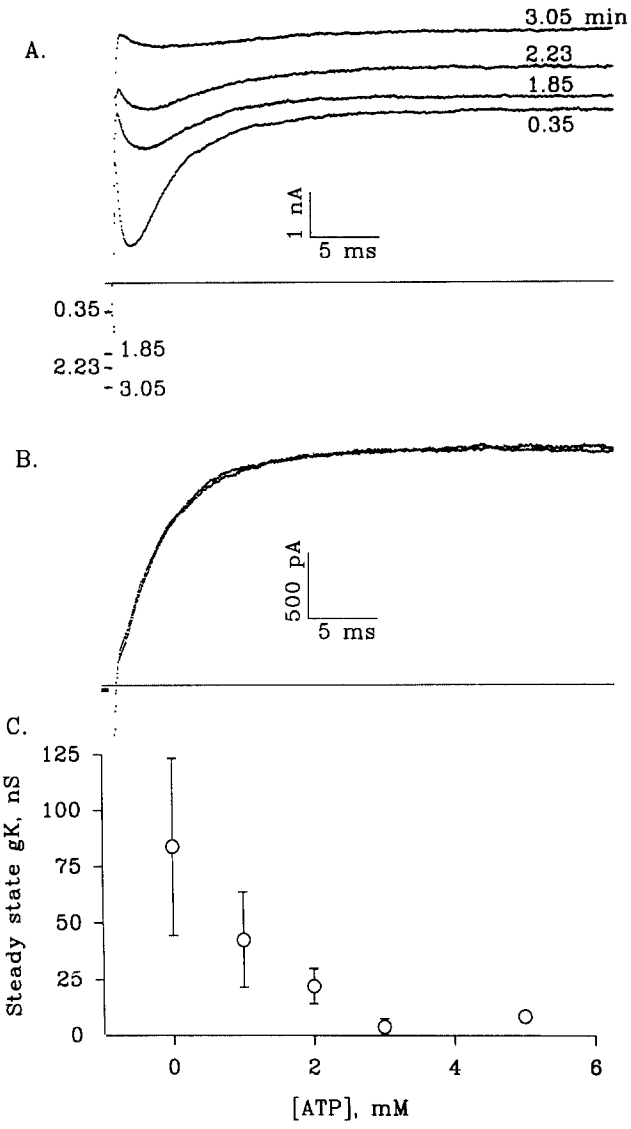

Fig. 6. K currents recorded with the classical whole-cell variation of the patch-clamp technique. (*A*) Currents obtained in response to 37 msec pulses to +70 mV with no ATP in the pipette. The time after breaking into the cell is given next to each trace. The holding current and the steady-state component of the outward current both increase with time. (*B*) Whole cell K currents recorded with 4 mM ATP in the pipette, using the same pulse pattern as in *A*. Two currents are shown: one recorded immediately after break-in and the other one 30 min later. Note that there is no change in the holding current or the outward current when ATP is included in the pipette. (*C*) Steady state g_K is plotted *vs.* the concentration of ATP in the pipette, showing that the conductance is sensitive to intracellular [ATP]. Data are plotted as mean ± SD. Solutions used were external solution A and internal solution F

steady-state g_K is due to the loss of ATP through the patch electrode, as suggested by the results of Fig. 6*B*, which show that in the presence of 4 mM ATP in the pipette there is no increase in g_K after 30 min (Fig. 6*B*). The magnitude of the steady-state g_K decreases with increasing concentrations of ATP in

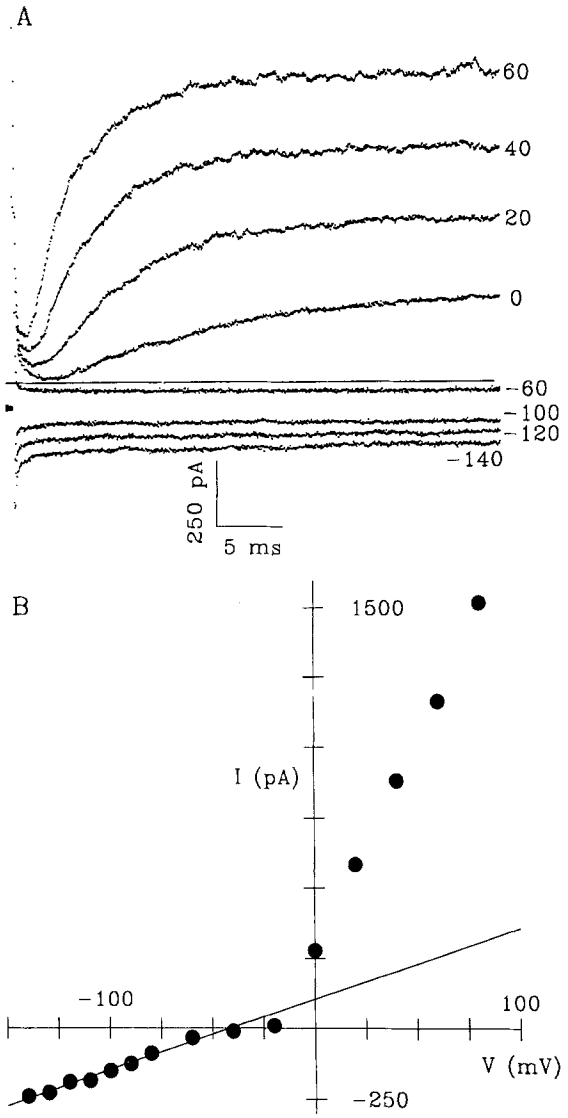

Fig. 7. K currents recorded with the perforated patch configuration. (A) Family of records obtained with 37 msec steps to the indicated potentials. Voltages positive to −20 mV activated voltage-dependent outward potassium current. At negative voltages, an inward time-independent current was evident. (*B*) Peak *I-V* relationship obtained from the records shown in *A*. The straight line fit to the inward currents yielded a steady-state conductance of 2.52 nS and a reversal potential of −41.5 mV. Solutions used were external solution A and internal solution E

the pipette (Fig. 6*C*), suggesting that this conductance is due to K_{ATP} channels. The maximum K_{ATP} conductance, measured in the absence of ATP, was 83.8 ± 40 nS (n = 12), and it provides a measure of the maximum number of K_{ATP} channels in the cell.

Perforated Patch Recordings and the Resting K_{ATP} Conductance

Using perforated patch recordings, internal ATP cannot leave the cell, and therefore the magnitude of the *resting* K_{ATP} conductance can be measured. The family of records in Fig. 7*A* were obtained in the nystatin perforated patch configuration after the access resistance had stabilized. The outward currents are clearly voltage dependent, activating faster at more depolarized voltages and are caused by voltage-dependent K (K_v) channels. The inward currents do not show any voltage or time dependence. A plot of the maximum current as a function of the pulse voltage is shown in Fig. 7*B*. Between −140 and −60 mV the *I-V* relationship is linear and reverses at −41 mV, near the expected E_K. In 13 cells, this steady-state inward K conductance averaged 3.57 ± 2.09 nS. This conductance gives a measure of the number of K_{ATP} channels open at rest. By dividing this steady-state K_{ATP} conductance in the intact cell by the maximum K_{ATP} conductance we estimate that only about 4% of the K_{ATP} channels are open.

Glyburide Block of K_{ATP}

It has previously been shown that sulfonylureas, like glyburide, are selective blockers of K_{ATP} channels in pancreatic β-cells (Sturgess et al., 1985; Trube, Rorsman & Ohno-Shosaku, 1986), so we have tested its effect on the steady-state g_K to provide additional evidence that K_{ATP} channels carry this current. The inset in Fig. 8*A* shows currents generated by 37 msec steps to −100 mV with (open circles) and without (filled circles) 10 μM glyburide. The holding current and the current during the pulse are both attenuated in the presence of glyburide. The *I-V* shows that the steady-state g_K, in the range of −120 to −40 mV, decreased from 2.46 to 0.08 nS upon addition of glyburide. Similar results were obtained in four other cells. Glyburide has a much smaller effect on K_v channels, as shown in Fig. 8*B*. The outward current at +70 mV decreased by 10% after applying glyburide. These experiments confirm that K_{ATP} channels are responsible for the majority of the steady-state g_K.

Pinacidil Enhances K_{ATP} Conductance

The steady-state g_K can be enhanced by the application of pinacidil, a K_{ATP} channel opener (Arena & Kass, 1989). The inward current generated by a step to −120 mV increased about 4.3 times in the presence of 500 μM pinacidil, and the effect was reversible (Fig. 9*A*). In the experiment of Fig. 9, the control g_K was 5.11 nS, and it increased to 28.1 nS after being exposed to 500 μM pinacidil for 15 min, and then returned to 6.48 nS after washing out the drug.

Comparison of K_v Kinetics in Whole Cell versus Perforated Patch

As an additional check on the accuracy of perforated patch recordings, we have compared activation ki-

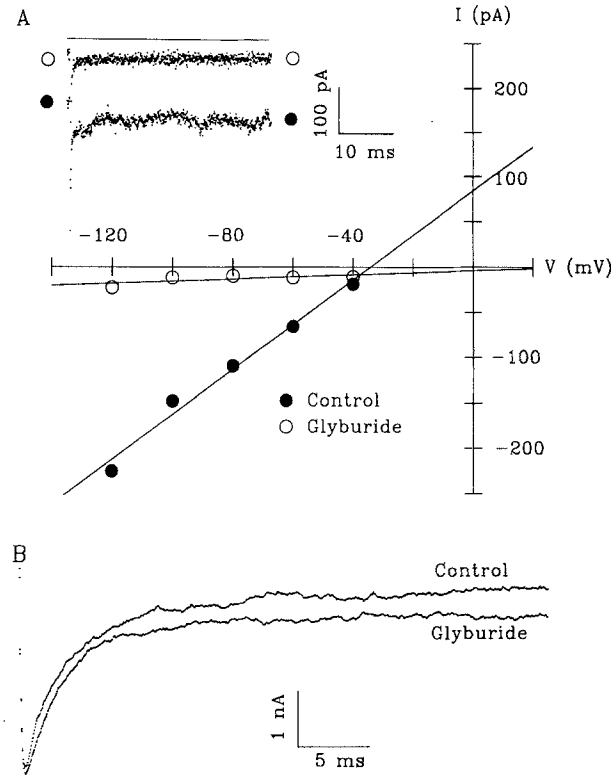

Fig. 8. (*A*) Glyburide block of K_{ATP} currents in a nystatin perforated patch experiment. Currents were obtained in respone to 37 msec pulses to various potentials, and the inset illustrates traces at −100 mV. *I-V* relationships were obtained after the access resistance had stabilized (control, filled circles) and then 2 min after the introduction of 10 μM glyburide (open circles). The steady-state potassium conductance decreased from 2.46 nS in control to 0.08 nS after adding glyburide. Immediately after sealing, before any nystatin effect was seen, an identical *I-V* was applied to measure the seal resistance. The conductance obtained by this *I-V* was subtracted from subsequent *I-V*'s. (*B*) Voltage-dependent K currents generated in response to 37 msec steps to +70 mV. There is only a 10% decrease in the current after 4 min in 10 μM glyburide. Solutions were external solution A and internal solution E

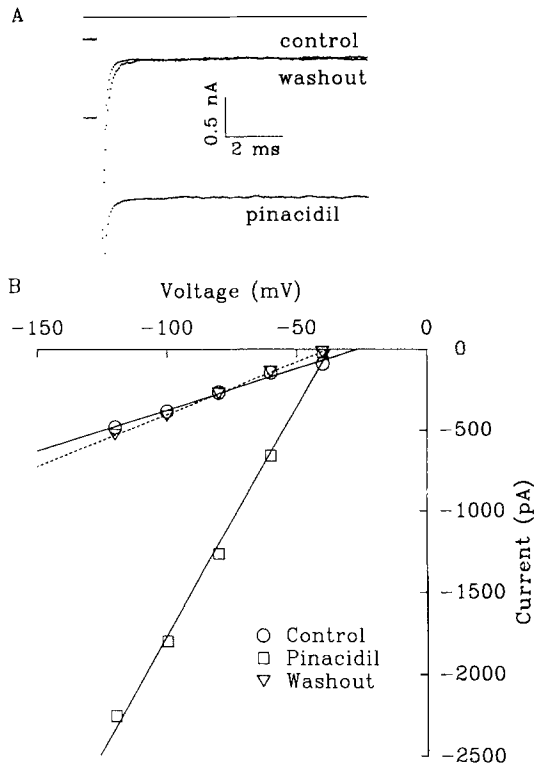

Fig. 9. Pinacidil activation of steady-state K conductance. (*A*) Currents recorded during 37 msec steps to −120 mV before (control), during (pinacidil) and after application of 500 μM pinacidil. Pinacidil increased the holding current and the magnitude of the current during the pulse. (*B*) *I-V* relationships obtained from currents generated by 37 msec steps to various voltages. The steady-state K conductance, estimated from straight line fits to the data, was 5.11 nS in control, 28.1 nS in pinacidil and decreased to 6.48 nS after washout. Solutions used were external solution A and internal solution E

netics of K_v currents obtained in whole cell mode with perforated patch recordings. The time to half maximal outward current ($t_{1/2}$) was used as a measure of the activation kinetics. When using the whole-cell configuration, the rate of K_v channel activation increases over the first 10 min of recording and then stabilizes. In Fig. 10, the $t_{1/2}$ *vs.* voltage curve taken 15 min after break-in (filled circles) is shifted in the hyperpolarizing direction relative to the curve taken immediately after break-in (open circles). This result is similar to previous reports of a shift in voltage-dependence as a function of time in whole-cell recordings and has been attributed to the rundown of a Donnan potential caused by large, relatively immobile intracellular anions (Marty & Neher, 1983; Fernandez et al., 1984). If a dissipating Donnan potential causes the shift, then kinetic measurements obtained with the perforated patch should agree with the late whole cell recordings, because the Donnan potential is very small in the perforated patch configuration (*see* Materials and Methods). Figure 10 in fact illustrates that the K_v activation kinetics in perforated patch are nearly identical to the late whole cell data. Figure 10*B* shows that when the perforated patch and late whole cell data are shifted 27 mV in the depolarizing direction, they agree quantitatively with the early whole-cell data.

Discussion

In many respects, channel studies involving whole-cell measurements of ionic currents are easier to perform and analyze than single channel recordings.

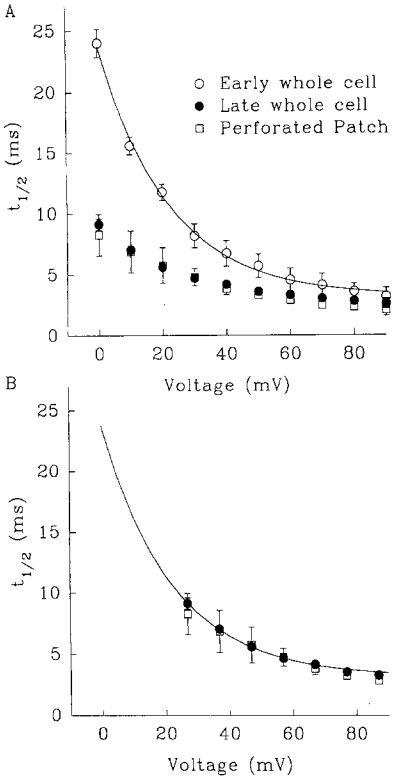

Fig. 10. Activation kinetics of K_v currents in whole cell *versus* perforated patch. (*A*) Currents were recorded during 37 msec pulses to voltages in the range 0 to 90 mV. The time to half-maximum current ($t_{1/2}$) was measured, and is plotted *vs.* voltage. In whole cell experiments, leak-subtracted currents were obtained immediately after break-in (open circles) and 15 min later (filled circles). Similar measurements were made using the perforated patch configuration after the access resistance had stabilized. The smooth curve is the fit of a single exponential to the early whole cell data. Each symbol is the mean ± SD (n = 3). (*B*) The smooth curve is the same exponential as in (*A*), and the filled circles and open squares are the late whole cell and perforated patch data shifted by +27 mV. Solutions used were external solution A, internal solution F with 4 mM ATP for the whole cell data, and solution E for the nystatin data

However, there are a number of limitations associated with the whole-cell variation of the patch-clamp technique. In this configuration, the dialysis of the cell interior against the contents of the patch electrode can have many effects: e.g., the loss of responsiveness to receptor-coupled second-messenger systems, rundown of Ca currents, or slow shifts in voltage-dependent parameters. The perforated-patch configuration presents a possible solution to these problems. It offers a method of whole-cell recording without dialysis by perforating the membrane under the electrode tip with monovalent selective channels. However, because of the potentially high access resistance between the pipette and the cell interior, the time resolution in this patch-clamp configuration will be less than that possible with the classical whole-cell variation. It has not yet been shown that this technical limitation can be overcome, so that rapid, voltage-dependent ionic currents, like fast Ca tail currents, can be measured accurately. We have now shown that within these technical limitations the technique can in fact be used to accurately resolve Ca tail currents and K_v activation kinetics.

Importance of Monitoring the Access Resistance

As seen in Figs. 2 and 3, the outward K current and the inward Ca current increase in magnitude as R_a decreases. This change in current magnitude most likely results from a decrease of the series resistance, which in this configuration is $R_n + R_p$ (*see* Fig. 1). For example, in the case of the K currents, the voltage drop caused by current flowing through $R_n + R_p$ would decrease the membrane voltage below the command voltage (V_c). This would decrease the driving force on K^+ and thus the magnitude of the K current. In the experiment illustrated in Fig. 2, the early K current (in the presence of a high R_a) generated by a V_c to +70 mV has about the same magnitude as the later K current (with low R_a) in response to a V_c to +10 mV. Thus, the larger R_a at the earlier time produced a larger series resistance error and a smaller K current. By monitoring R_a as nystatin perforations develop, its steady-state magnitude can be determined and series resistance compensation set appropriately.

Another reason for carefully following R_a concerns sudden changes which sometimes occur. For example, while we have observed Ca currents without rundown for over 90 min, we have also occasionally seen rundown of Ca currents that starts at almost any time during an experiment. This is often accompanied by a small decrease in R_a suggesting that it is due to a spontaneous break-in. This effect is easy to document with periodic estimates of R_a.

Ca Tail Currents

Macroscopic currents have been used to characterize multiple types of Ca channels in various cells (Carbone & Lux, 1984; Armstrong & Matteson, 1985; Nowycky, Fox & Tsien, 1985) including pancreatic β-cells (Hiriart & Matteson, 1988). One of the most accurate ways of distinguishing between the Ca channel subtypes using whole-cell recordings has been with tail currents (Matteson & Armstrong,

1986; Cota, 1986; Carbone & Lux, 1987; Cohen et al., 1988; Satin & Cook, 1988; Chen & Hess, 1990). In order to use the perforated patch technique to study Ca channel subtypes, we had to demonstrate our ability to resolve tail currents with this technique. In experiments with sufficiently low τ_a, two components of the tails were easily distinguished. Conductance-voltage relationships obtained with the perforated patch measurements were comparable to those found in whole cell experiments (Fig. 5), demonstrating that under appropriate conditions, perforated patch can be used to accurately study multiple components of Ca tail currents.

Activation Kinetics and the Donnan Potential

Marty and Neher (1983) were the first to predict that a slowly dissipating liquid junction potential could form at the tip of a patch pipette after establishing a whole-cell recording, due to relatively immobile anions in the cell. This Donnan potential, which would make the cell interior more negative than the pipette, would decrease in time as the anions diffuse out of the cell, leading to a slow change in the membrane potential in spite of a constant command potential. Subsequently, there were several reports of slow shifts in the voltage dependence of various channel properties which were attributed to a Donnan potential which decreased with time (Fernandez et al., 1984; Cahalan et al., 1985; Cota, 1986). Our results with the perforated patch configuration support this idea. Using the whole-cell configuration of the patch clamp we found that K_v activation kinetics became faster with time after break in, consistent with a dissipating Donnan potential. In perforated patch experiments, the pipette solution was designed to minimize the Donnan potential (*cf.* Materials and Methods and Horn & Marty, 1988), so these measurements should be similar to the late whole cell measurements. Figure 10 shows that this was, in fact, the case. These results also demonstrate that the perforated patch configuration can be used to accurately measure K_v activation kinetics.

K_{ATP} Resting Conductance in β-Cells

There is evidence that modulation of K_{ATP} channel activity is responsible for glucose induced electrical activity in pancreatic β-cells (Ashcroft, 1988). Furthermore, it is believed that intracellular ATP is the physiological regulator of the channel. However, single channel studies have demonstrated a high affinity block of the channels by ATP (K_I = 0.015 mM: Cook & Hales, 1984), so that in the presence of millimolar concentrations of ATP in the cell nearly all of the channels would be blocked. Several explanations have been offered to explain this apparent discrepancy. For example, one possibility is that very few K_{ATP} channels are, in fact, open in the intact β-cell, and closure of only a few channels depolarizes the cell to threshold (Cook et al., 1988). Another factor is that the apparent K_I for ATP block of the channel is increased in the presence of physiological concentrations of ADP. For example, Kakei et al. (1986) report that in the presence of 2 mM ADP the K_I for ATP increases to 0.145 mM. Because of these considerations we wanted to estimate the fraction of open K_{ATP} channels in the intact cell to see if it was consistent with known intracellular concentrations of ATP and ADP. Prior to the development of the perforated patch technique the only noninvasive method of recording K_{ATP} channel activity used on-cell single channel recording (e.g. Ashcroft, Harrison & Ashcroft, 1984), and with this configuration it was not possible to estimate the fraction of open channels. We have now shown that stable recordings of K_{ATP} channels can be obtained from the entire cell surface with the perforated patch configuration, allowing us to study the average activity of a large number of K_{ATP} channels in an intact β-cell. By comparing the steady-state g_K measured in perforated patch experiments with classical whole-cell recordings obtained in the absence of intracellular ATP, we have estimated that only about 4% of the β-cell's K_{ATP} channels are open in the absence of extracellular glucose. With a K_I of 0.145 mM (i.e., in the presence of 2 mM ADP), 4% of the channels would be open at an ATP concentration of 3.5 mM, which is close to that found experimentally (Kakei et al., 1986).

References

Arena, J.P., Kass, R.S. 1989. Enhancement of potassium-sensitive current in heart cells by pinacidil. *Circ. Res.* **65**:436–445

Armstrong, C.M., Bezanilla, F. 1974. Charge movement associated with the opening and closing of the activation gates of the Na channel. *J. Gen. Physiol.* **63**:533–552

Armstrong, C.M., Matteson, D.R. 1985. Two distinct populations of calcium channels in a clonal line of pituitary cells. *Science* **227**:65–67

Ashcroft, F.M. 1988. Adenosine 5′-triphosphate-sensitive potassium channels. *Annu. Rev. Neurosci.* **11**:97–118

Ashcroft, F.M., Harrison, D.E., Ashcroft, S.J.H. 1984. Glucose induces closure of single potassium channels in isolated rat pancreatic B-cells. *Nature* **312**:446–448

Ashcroft, F.M., Kakei, M., Kelly, R.P. 1989. Rubidium and sodium permeability of the ATP-sensitive K^+ channel in single rat pancreatic beta-cells. *J. Physiol.* **408**:413–429

Ashcroft, F.M., Kelley, R.P., Smith, P.A. 1990. Two types of Ca channel in rat pancreatic B-cells. *Pfluegers Arch.* **415:**504–506

Cahalan, M.D., Chandy, K.G., DeCoursey, T.E., Gupta, S. 1985. A voltage-gated potassium channel in human T-lymphocytes. *J. Physiol.* **358:**197–237

Carbone, E., Lux, H.D. 1984. A low voltage activated, fully inactivating Ca channel in vertebrate sensory neurones. *Nature* **310:**501–511

Carbone, E., Lux, H.D. 1987. Kinetics and selectivity of a low-voltage-activated calcium current in chick and rat sensory neurones. *J. Physiol.* **386:**547–570

Chen, C., Hess, P. 1990. Mechanisms of gating of T-type calcium channels. *J. Gen. Physiol.* **96:**603–630

Cohen, A.S., Matteson, D.R., Parsey, R.V., Sala, S. 1990. Ionic currents in rat pancreatic beta cells recorded with the perforated patch technique. *Biophys. J.* **57:**509*a*

Cohen, C.J., McCarthy, R.T., Barrett, P.Q., Rasmussen, H. 1988. Ca channels in adrenal glomerulosa cells: K^+ and angiotensin II increase T-type Ca channel current. *Proc. Natl. Acad. Sci. USA* **85:**2412–2416

Cook, D.L., Hales, C.N. 1984. Intracellular ATP directly blocks K^+ channels in pancreatic B-cells. *Nature* **311:**271–273

Cook, D.L., Satin, L.S., Ashford, M.L.J., Hales, C.N. 1988. ATP-sensitive K^+ channels in pancreatic β-cells. *Diabetes* **37:**495–498

Cota, G. 1986. Calcium channel currents in pars intermedia cells of the rat pituitary gland. *J. Gen. Physiol.* **88:**83–105

Falke, L.C., Gillis, K.D., Pressel, D.M., Misler, S. 1989. 'Perforated patch recording' allows long-term monitoring of metabolite-induced electrical activity and voltage-dependent Ca^{2+} currents in pancreatic islet B cells. *FEBS Lett.* **251:**167–172

Fernandez, J.M., Fox, A.P., Krasne, S. 1984. Membrane patches and whole-cell membranes: A comparison of electrical properties in rat clonal pituitary (GH3) cells. *J. Physiol.* **356:**565–585

Hagiwara, S., Byerly, L. 1983. The calcium channel. *Trends Neurosci.* **6:**189–193

Hamill, O.P., Marty, A., Neher, E., Sakmann, B., Sigworth, F.J. 1981. Improved patch-clamp techniques for high-resolution current recording from cells and cell-free membrane patches. *Pfluegers Arch.* **391:**85–100

Hiriart, M., Matteson, D.R. 1988. Sodium channels and two types of calcium channels in rat pancreatic beta cells identified with the reverse hemolytic plaque assay. *J. Gen. Physiol.* **91:**617–639

Horn, R., Marty, A. 1988. Muscarinic activation of ionic currents measured by a new whole-cell recording method. *J. Gen. Physiol.* **92:**145–159

Kakei, M., Kelly, R.P., Ashcroft, S.J.H., Ashcroft, F.M. 1986. The ATP-sensitivity of K^+ channels in rat pancreatic B-cells is modulated by ADP. *FEBS Lett.* **208:**63–66

Korn, S.J., Horn, R. 1989. Influence of sodium-calcium exchange on calcium current rundown and the duration of calcium-dependent chloride currents in pituitary cells, studied with whole cell and perforated patch recording. *J. Gen. Physiol.* **94:**789–812

Kurachi, Y., Asano, Y., Takikawa, R., Sugimoto, T. 1989. Cardiac Ca current does not run down and is very sensitive to isoprenaline in the nystatin method of whole cell recording. *Naunyn-Schmiedeberg's Arch. Pharmacol.* **340:**219–222

Lindau, M., Fernandez, J.M. 1986. IgE-mediated degranulation of mast cells does not require opening of ion channels. *Nature* **319:**150–153

Lucero, M.T., Pappone, P.A. 1990. Membrane responses to NE in cultured brown fat cells. *J. Gen. Physiol.* **95:**523–544

Marty, A., Neher, E. 1983. Tight-seal whole-cell recording. *In:* Single Channel Recording. B. Sakmann and E. Neher, editors. pp. 107–122. Plenum, New York

Matteson, D.R., Armstrong, C.M. 1986. Properties of two types of calcium channels in clonal pituitary cells. *J. Gen. Physiol.* **87:**161–182

Nowycky, M.C., Fox, A.P., Tsien, R.W. 1985. Three types of neuronal calcium channels with different calcium agonist sensitivity. *Nature* **316:**440–443

Rorsman, P., Trube, G. 1986. Calcium and delayed potassium currents in mouse pancreatic β-cells under voltage clamp conditions. *J. Physiol.* **374:**531–550

Sala, S., Matteson, D.R. 1990. Single-channel recordings of two types of calcium channels in rat pancreatic β-cells. *Biophys. J.* **58:**567–571

Satin, L.S., Cook, D.L. 1988. Evidence for two calcium currents in insulin-secreting cells. *Pfluegers Arch.* **411:**401–409

Sturgess, N.C., Ashford, M.L.J., Cook, D.L., Hales, C.N. 1985. The sulfonylurea receptor may be an ATP-sensitive potassium channel. *Lancet* **8453:**474–475

Trube, G., Rorsman, P., Ohno-Shosaku, T. 1986. Opposite effects of tolbutamide and diazoxide on the ATP-dependent K^+ channel in mouse pancreatic β-cells. *Pfluegers Arch.* **407:**493–499

Received 30 November 1990; revised 28 January 1991